International Journal of GEOMATE, May, 2020, Vol.18, Issue 69, pp. 130 - 135
ISSN: 2186-2982 (P), 2186-2990 (O), Japan, DOI: https://doi.org/10.21660/2020.69.9427
Geotechnique, Construction Materials and Environment

FTIR AND UV IN STEEL PIPELINE COATING APPLICATION

Omar Abdelkarim[1], Mohamed Hazem Abdellatif[1], Diaa Khalil[1], and Ghada Bassioni[1]

[1] Faculty of Engineering, Ain Shams University, Cairo, Egypt

*Corresponding Author, Received: 29 June 2019, Revised: 01 Dec. 2019, Accepted: 08 Feb. 2020

ABSTRACT: Different spectrum can be used in characterization and upsetting the performance of our daily application. Fourier transform infrared (FTIR) spectroscopy is used to make structural analysis for materials. The need to have low cost, portable, and suitable size FTIR to be used onsite application is in need. A novel microelectromechanical system (MEMS)-based FTIR spectrometer device is made to solve this problem. Epoxy coating is used frequently to protect steel pipelines from environmental conditions against corrosion. Its drawback is that it performs with low resistance for crack initiation and propagation. In addition, the absorption of ultraviolet radiation (UV) deteriorates its properties. Which reduces the lifetime of the coating. Having direct and indirect economic losses. The usage of alumina nanoparticles with a small amount of weight percentage of 0.25 wt. % can enhance mechanical properties. The key factor is having a good distribution of nanoparticles inside the epoxy-resin matrix. The investigation of the mechanical properties, bulk properties as in flexural strength, and surface properties as in erosion resistance and hardness are studied. Furthermore, the effect of 48 h UVA absorption on the performance of these properties with different alumina nanoparticles wt. % is investigated. For the bulk properties, the addition of alumina nanoparticles having an insignificant effect, while in surface properties, the effect of UV reduces with the increase in particle wt. %. The MEMS-FTIR has good agreement with mechanical properties. Indicating the distribution of particles inside the system. Supported by environmental scanning electron microscope (ESEM) images. This shows that MEMS-FTIR is a useful instrument used in non-destructive, low cost, onsite material analysis.

Keywords MEMS-FTIR - Epoxy resin · Alumina nanoparticles · Coating - Mechanical properties

1. INTRODUCTION

Spectroscopy is an important characterization technique that analyzes the interaction between matter and electromagnetic spectrum [1]. There are different types of spectroscopy, with a wide range of electromagnetic wavelengths, ranging from Gamma rays to radio waves [2-8]. Fourier transform infrared (FTIR) spectroscopic analysis is one way to analyze the structure of different materials [9-12]. The use of portable, low cost, average size near-infrared spectroscopy (NIRS) as a non-destructive testing technique is a major challenge. One way to solve this problem is by using a microelectromechanical system (MEMS)-based FTIR spectrometer [13]. This device can be used for practical applications, onsite material analysis, which can save cost and time.

Steel pipeline manufacturing has been developed in the last decades [14]. Continuously increasing the strength of pipeline, reducing its thickness that decreases the overall cost has been of major concern. A challenge remains corrosion of steel that depends on environmental and operational factors [15]. Many ways are used for protection including surface coating, which acts as a barrier between the steel and the environment [16-19]. Liquid epoxy coating is one type that is widely used, because of a good electrical insulator, adhesion, chemical, and mechanical properties [20-26]. A drawback for epoxy coating is that it has a poor resistance for crack initiation and propagation, and surface damage through abrasion ware [27]. Furthermore, epoxy degrades when it is exposed to sunlight for a long time, due to the absorption of ultraviolet radiation (UV) [28]. This degradation deteriorates the mechanical and physical properties [29-31], eventually causing direct and indirect economic losses [32].

Incorporation of nanoparticles in epoxy systems can enhance the properties at the nanoscale. The factors that affect the properties are matrix-to-particle interaction and particle-to-particle interaction [33]. Nanoparticles with a high surface to volume ratio tend to reduce its surface energy by interacting with each other to form agglomerates, which deteriorate the properties [34]. This interaction can be controlled through particle disruption, loading, and shape. The interface between matrix and particles, its quality enhances load transfer to nanoparticles, which enhances the mechanical properties [35].

In this study, two different spectra are used to investigate a system composed of epoxy resin with alumina nanoparticles with different weight percentages (wt. %). The effect of ultraviolet radiation A (UVA), which is the main cause of epoxy degradation, on the mechanical and physical properties, and MEMS-based FTIR spectroscopy used for material characterization.

2. EXPERIMENTAL

Alumina nanoparticles are used due to high phase and dimensional stability, commercial availability, and hardness. The particles wt. % used are (0 – 0.25 – 0.5 – 0.75 – 1). The UVA exposure is for 48 hours for each sample. The detection of alumina nanoparticles distributed in the epoxy-resin matrix in the near-infrared (NIR) range using an on-chip silicon micro-electro-mechanical for the application of coating steel pipelines is also studied.

2.1 Materials

KEMAPOXY epoxy-resin, mixing ratio 2:1 (resin: hardener), bought from CMB. α alumina nanoparticles, coated with aluminic ester, with 60 nm particle size, superhydrophobic, bought from US research nanomaterial, Inc.

2.2 Mold preparation

Silicon rubber mold is prepared according to ASTM D790. Using steel samples, with the same dimensions as the standard sample, as a positive pattern, then pouring silicon rubber mixture to cure on theses samples, providing the mold used for epoxy-resin/alumina nanoparticles composite samples. The ratio between resin and hardener for silicon rubber is 950:32. A vacuum pump is used to remove any air bubbles inside for 10 min. then poured over the steel samples.

2.3 Sample preparation

The epoxy resin is weighed, heated to 50ºC for 10 min to decrease the viscosity, and evacuated from any air bubbles through a vacuum pump for 30 min. Then alumina nanoaparticles with different wt. % are weighed, using sensitive scale, and added to the epoxy resin. The mixture is then stirred, using a magnetic stirrer, for 1 h. Subsequently evacuated for 30 min using a vacuum pump. Then the hardener is added to the mixture, stirred for 15 min, evacuated for 5 min, and finally poured into the silicon rubber mold. The nanocomposite is left to cure at room temperature for 24 h, then post-curing at 80ºC for 16 h. The samples are then exposed to an ultraviolet lamp, in a sealed chamber, for 48 h at room temperature.

2.3 Characterization

2.3.1 MEMS-FTIR

The spectrum reflected by the samples is measured using the MEMS FTIR spectrometer. Spectralon (diffuse reflectance standard) is used as a background, and samples reflectance are measured with respect to it. All measurements are taken with 10 sec averaging time and a resolution of 16 nm. Samples with different concentrations are measured. For each concentration, different positions are tested to identify variation in nanoparticles distribution in the sample. The sample was placed on the source with free-space above to ensure no reflection from objects. The sample was coupled in the spectrometer’s fiber.

2.3.2 ESEM

ESEM (Quanta FEG250) is used to take images for the cross-section of alumina/epoxy nanocomposite. Sample size $1\ cm * 1\ cm * 0.4\ cm$ is used. Samples are gold plated first to enhance the conductivity.

2.3.2 Mechanical properties

Bending test: A 3-point bending test is used to test epoxy-resin and alumina/epoxy nanocomposites. The load is applied to the middle of specimens, supported by 2 spans. ASTM D790 (2004) specimens’ specification. The machine used is a 10 Ton LLYOD testing machine.

Erosion test: Sand erosion testing is performed on the samples. After projecting the samples to a stream of abrasive sand particles for 9 minutes, the weight of each sample is measured 9 times, each after 1 min, by sensitive scale, then the slope of the line is calculated as the erosion rate, which is converted to erosion resistance.

Hardness test: The same samples used for the bending test is used to measure the hardness of the composite. Each sample is tested 3 times, at 3 different locations. The test is performed using a ZWICK/ROELL testing instrument, to determine the hardness behavior at room temperature.

The prepared samples are subjected to Ultraviolet radiation, before being tested, investigating the effect of UV radiation on the composites. Using a self-assembled sealed chamber, consisting of 3 partitions, UVA, UVB, and UVC is used to expose the specimens to ultraviolet radiation UVA. The exposure duration to UVA is 48 h at room temperature.

3. RESULTS AND DISCUSSION

Nanoparticles distribution is analyzed using MEMS-FTIR spectroscopy. The spectrum of different concentrations and positions is shown in Fig. 1. The spectrum shows that for the 0.25 wt. % sample, the alumina nanoparticle distribution is well dispersed inside the matrix, no difference with different positions. As we increase the particle wt. %, the spectrum varies from one position to the other. The variation gradually increases as we increase the particle wt. % with the highest variation in 1 wt. %. These results indicate that agglomeration starts to occur as we increase the amount of alumina nanoparticles inside the epoxy-resin matrix as well as the uneven distribution of the nanoparticles inside the system.

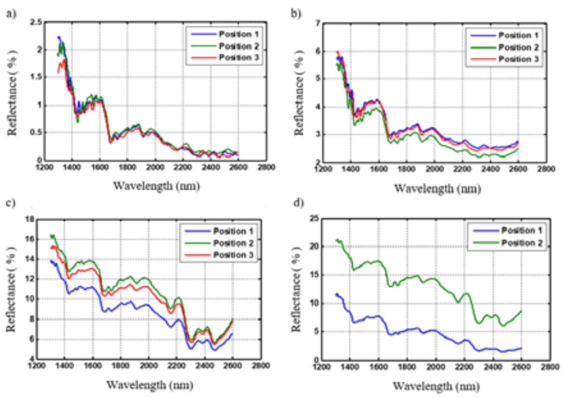

Fig. 1 MEMS-FTIR reflectance spectrum for a) 0.25 wt. % b) 0.5 wt. % c) 0.75 wt. % and d) 1 wt, % of alumina nanoparticles inside epoxy-resin matrix at different positions

The effect of increasing the amount of alumina nanoparticles wt. % on the spectrum is shown in Fig. 2. As we increase the amount of nanoparticles, the reflectance increases, from the wavelength of 1300 nm to 1700 nm, then at higher wavelength, there are insignificant changes. These results indicate that the more nanoparticles we add to the system, the more interaction bonds occur between the chains and these nanoparticles. These bonds hinder the movement of the polymer chains during the light exposure and hence increase the reflectance peak for the same wavelength.

The effect of UV on the reflectance spectrum varies from one concentration to another. For pure sample, without alumina nanoparticles, the spectrum shifts upwards, which indicate that the UV exposure increases the amount of crosslinking inside the system, and hinders the movement of chains. While for the samples with different alumina nanoparticles a different behavior is observed due to the inhomogeneous distribution of particles inside the matrix, as proven in Fig. 1.

ESEM micrographs of the cross-section of the samples are shown in Fig. 3. Those images support the results from MEMS-FTIR showing the

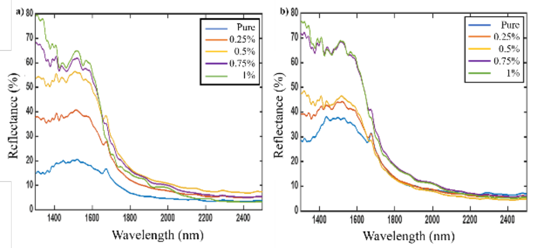

Fig. 2 Effect of particle wt. % on the MEMS-FTIR reflectance spectrum a) before UV exposure b) after UV exposure

agglomerations that occur in different particle wt. %, in the indicated white circles. The more the particles wt. %, the more agglomeration occurs. From Fig. 1 and Fig. 3, we can conclude that as the amount of nanoparticles increases in the system, more particle-to-particle interaction increases, and more agglomeration occurs.

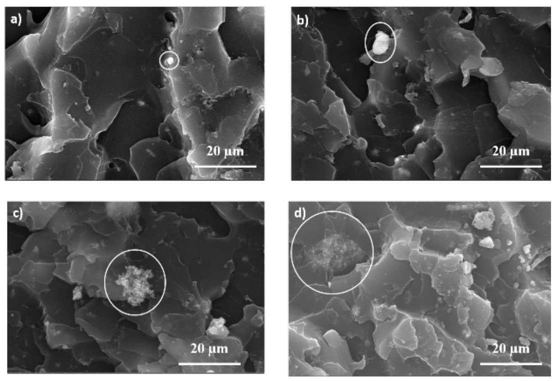

Fig. 3 ESEM microscopy of cross section surface at 20 µm of epoxy alumina nanoparticles composite with a) 0.25 wt. % b) 0.5 wt. % c) 0.75 wt. % and d) 1 wt. %

In order to investigate the effect of UVA exposure on the samples, different tests are performed: Three-point bending test, Hardness Test, and sand erosion test. All samples are subjected to these tests before and after UVA exposure. The effect of UVA for test results, comparing before and after UVA exposure, are summarized in table 1.

Table 1 Mechanical properties of epoxy resin reinforced with alumina nanoparticles, the difference between before and after exposure to UVA

Alumina Nanoparticles wt.%	Effect of UV on Flexural Strength (%)	Effect of UV on Erosion Resistance (%)	Effect of UV on Hardness (%)
0.00%	-1.11%	-23.0%	-20.4%
0.25%	1.11%	-19.8%	-16.9%
0.50%	-0.61%	-2.5%	-13.0%
0.75%	2.04%	-6.5%	-12.3%
1.00%	-5.06%	10.4%	0.8%

Flexural strength of epoxy-resin samples with different alumina nanoparticles, before and after exposure to UVA, is shown in Fig 4. The flexural strength increases in case of 0.25 wt. % with respect to pure sample with 7% from 77.1 MPa to 83.06 MPa. Then the strength gradually decreases with increasing wt. % till it reaches 62.45 MPa at 1 wt. %, which is 19% decrease compared to the pure sample. The reason for increasing the strength is due to the good dispersion of alumina nanoparticles inside the matrix. More particle to matrix interface occurs, which transfers more load from the matrix to the nanoparticles, carrying more load, and enhancing the strength of the system. However, a further increase in alumina wt. %, increases particle agglomeration, so more particle-to-particle interaction occurs. These agglomeration works as stress concentration parts, which initiate cracks inside the system, lowering its performance. MEMS-FTIR and ESEM in Fig 1 and 3 can be used as a support for this statement.

The difference between the flexural strength, before and after exposure to UVA, is shown in Fig. 4. From these data, there is an insignificant difference between the flexural strength before and after 48 h. UV exposure, as shown in table 1.

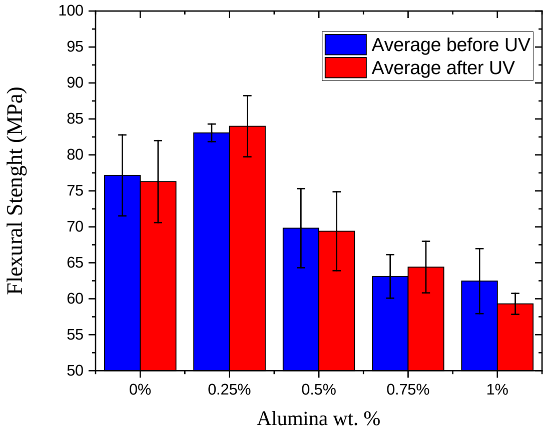

Fig. 4 Flexural strength of epoxy resin reinforced with alumina nanoparticles, before and after exposure to UVA

Erosion resistance of epoxy-resin samples with different alumina nanoparticles, before and after exposure to UVA, is shown in Fig. 5. Similar to flexural strength. The erosion resistance increases in case of 0.25 wt. % with respect to pure sample with 67% from 0.824 min/mg to 2.477 min/mg. Then the resistance gradually decreases with increasing wt. % till it reaches 1.23 min/mg at 1 wt. %, which is 49% increase compared to the pure sample. The crosslinking density increases with the increase in particle wt. %, with good dispersion then gradually decreases in case of agglomeration.

From table 1, the increase in alumina nanoparticles reduces the UV effect gradually as we increase the wt. %. Starting from 23% reduction in the pure sample to 10.4% improvement in 1 wt. %. These results show that the addition of alumina nanoparticles improves the surface properties of the coating against UV exposure.

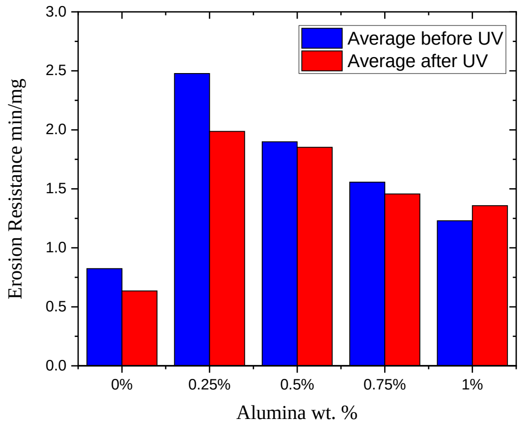

Fig. 5 Erosion resistance of epoxy resin reinforced with alumina nanoparticles, before and after exposure to UVA

The hardness of epoxy-resin samples with different alumina nanoparticles, before and after exposure to UVA, is shown in Fig. 6. In this case, The hardness slightly increases with the increase in particle addition. Starting with 75.6 Shore D for the pure sample. Until it reaches 79.3 Shore D for 0.75 wt. %, with 4.9% increase. For 1 wt. %, a reduction in Hardness occurs, due to inhomogeneous distribution of the nanoparticles, and the Hardness test is a localized test.

The effect of UV on the Hardness test is the same as in erosion resistance. As both are surface properties. The increase in alumina nanoparticles wt. % reduces the effect of UV gradually with the increase in wt. %. Staring from 20.4% reduction in pure sample to 0.8% improvement in 1 wt. %.

4. CONCLUSION

As a conclusion for this work, a novel MEMS-FTIR method is used to identify the alumina nanoparticles distributions, using different positions, for the same material, in an epoxy-resin matrix. These results are supported by ESEM micrographs. The mechanical properties of different alumina nanoparticles wt. % is investigated before and after UV exposure. For flexural strength, the properties improved with the

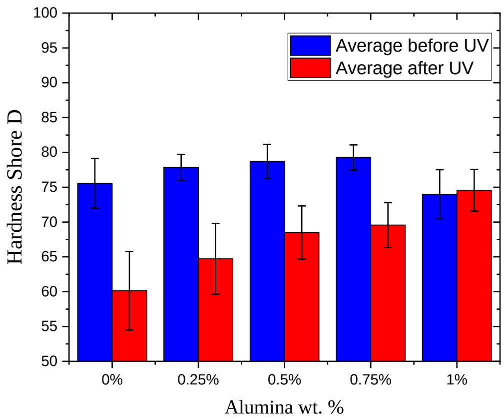

Fig. 6 Hardness Shore D of epoxy resin reinforced with alumina nanoparticles, before and after exposure to UVA

addition of 0.25 wt. % and reduced with increasing more of wt. which reduces crosslinking density and acts as stress concentration points. The erosion resistance properties follow the same trend as flexural strength, while hardness improves slightly with increasing particle wt. %. The effect of 48 h UV exposure is insignificant in flexural strength, indicating that the UV does not affect the bulk properties. On the other hand, in case of erosion resistance and hardness, as surface properties, the addition of alumina nanoparticles reduces the effect of UV with increasing the wt. %.

5. REFERENCES

[1] Harvey, D. Analytical Chemistry 2.0. 2016.

[2] Colthup, N. Introduction to infrared and Raman spectroscopy. Elsevier, 2012.

[3] Jensen, Traci R., George C. Schatz, and Richard P. Van Duyne. Nanosphere lithography: Surface plasmon resonance spectrum of a periodic array of silver nanoparticles by ultraviolet− visible extinction spectroscopy and electrodynamic modeling. The Journal of Physical Chemistry B, Vol. 103. Issue 13, 1999, pp. 2394-2401.

[4] Harris, R. K. Nuclear magnetic resonance spectroscopy. 1986.

[5] Gilmore, G. Practical gamma-ray spectroscopy. John Wiley & Sons, 2011.

[6] Briggs, D. ed. Handbook of X-ray and ultraviolet photoelectron spectroscopy. London: Heyden, 1977.

[7] Townes, Charles H., and Arthur L. Schawlow. Microwave spectroscopy. Courier Corporation, 2013.

[8] Gupta, S., Z. Hadzibabic, M. W. Zwierlein, C. A. Stan, K. Dieckmann, C. H. Schunck, E. G. M. Van Kempen, B. J. Verhaar, and W. Ketterle. Radio-frequency spectroscopy of ultracold fermions. Science, Vol. 300, Issue 5626, 2003, pp. 1723-1726.

[9] Schmitt, J., and Flemming, H. C. FTIR-spectroscopy in microbial and material analysis. International Biodeterioration & Biodegradation, Vol. 41, Issue 1, 1998, pp. 1-11.

[10] Colom, X., F. Carrillo, F. Nogués, and P. Garriga. Structural analysis of photodegraded wood by means of FTIR spectroscopy. Polymer degradation and stability, Vol. 80, Issue 3, 2003, pp. 543-549.

[11] Baker, M.J., Trevisan, J., Bassan, P., Bhargava, R., Butler, H.J., Dorling, K.M., Fielden, P.R., Fogarty, S.W., Fullwood, N.J., Heys, K.A. and Hughes, C. Using Fourier transform IR spectroscopy to analyze biological materials. Nature protocols, Vol. 9, Issue 8, 2014, pp.1771-1791.

[12] Rehman, Ihtesham, and W. Bonfield. Characterization of hydroxyapatite and carbonated apatite by photo acoustic FTIR spectroscopy. Journal of Materials Science: Materials in Medicine, Vol. 8, Issue 1, 1997, pp. 1-4.

[13] Khalil, D. A., Mortada, B., Nabil, M., Medhat, M., & Saadany, B. A. 2013. U.S. Patent No. 8,531,675. Washington, DC: U.S. Patent and Trademark Office.

[14] Kagechika, H. Recent progress and future trends in the research and development of steel. NKK Technical Review (Japan), Vol, 88, 2003, pp. 6-9.

[15] Banach, J. Liquid epoxy coatings for today's pipeline coating challenges. In Proceedings of Northern Area Western Conference, Victoria. 2004.

[16] Caporali, S., Fossati, A., Lavacchi, A., Perissi, I., Tolstogouzov, A., & Bardi, U. Aluminium electroplated from ionic liquids as protective coating against steel corrosion. Corrosion Science, Vol. 50, Issue 2, 2008, pp. 534-539.

[17] Shen, G. X., Y. C. Chen, and C. J. Lin. Corrosion protection of 316 L stainless steel by a TiO2 nanoparticle coating prepared by sol–gel method. Thin Solid Films, Vol. 489, Issue 1-2, 2005, pp. 130-136.

[18] Sathiyanarayanan, S., S. Syed Azim, and G. Venkatachari. A new corrosion protection

coating with polyaniline–TiO2 composite for steel. Electrochimica Acta, Vol. 52, Issue 5, 2007, pp. 2068-2074.

[19] Sathiyanarayanan, S., S. Muthukrishnan, G. Venkatachari, and D. C. Trivedi. Corrosion protection of steel by polyaniline (PANI) pigmented paint coating. Progress in Organic Coatings, Vol. 53, Issue 4, 2005, pp. 297-301.

[20] Behzadnasab, M., S. M. Mirabedini, K. Kabiri, and S. Jamali. Corrosion performance of epoxy coatings containing silane treated ZrO2 nanoparticles on mild steel in 3.5% NaCl solution. Corrosion Science, Vol. 53, Issue 1, 2011, pp. 89-98.

[21] Talo, A., P. Passiniemi, O. Forsen, and S. Yläsaari. Polyaniline/epoxy coatings with good anti-corrosion properties. Synthetic Metals, Vol. 85, No. 1-3, 1997, pp. 1333-1334.

[22] Shi, X., Nguyen, T. A., Suo, Z., Liu, Y., & Avci, R. Effect of nanoparticles on the anticorrosion and mechanical properties of epoxy coating. Surface and Coatings Technology, Vol. 204, Issue 3, 2009, pp. 237-245.

[23] Manning, David G. Corrosion performance of epoxy-coated reinforcing steel: North American experience. Construction and Building Materials, Vol. 10, Issue 5, 1996, pp. 349-365.

[24] Hang, T. T. X., Truc, T. A., Nam, T. H., Oanh, V. K., Jorcin, J. B., & Pébère, N. Corrosion protection of carbon steel by an epoxy resin containing organically modified clay. Surface and Coatings Technology, Vol. 201, No. 16-17, 2007, pp. 7408-7415.

[25] Shao, Y., Jia, C., Meng, G., Zhang, T., & Wang, F. The role of a zinc phosphate pigment in the corrosion of scratched epoxy-coated steel. Corrosion Science, Vol. 51, Issue 2, 2009, pp. 371-379.

[26] Galliano, F., and D. Landolt. Evaluation of corrosion protection properties of additives for waterborne epoxy coatings on steel. Progress in Organic Coatings, Vol. 44, Issue 3, 2002, pp. 217-225.

[27] Spanoudakis, J., and R. J. Young. Crack propagation in a glass particle-filled epoxy resin. Journal of Materials Science, Vol. 19, Issue 2, 1984, pp. 473-486.

[28] Singh, B., & Sharma, N. Mechanistic implications of plastic degradation. Polymer degradation and stability, Vol. 93, Issue 3, 2008, pp. 561-584.

[29] Joseph, P. V., Marcelo S. Rabello, L. H. C. Mattoso, Kuruvilla Joseph, and Sabu Thomas. Environmental effects on the degradation behaviour of sisal fibre reinforced polypropylene composites. Composites Science and Technology, Vol. 62, No. 10-11, 2002, pp. 1357-1372.

[30] Woo, R. S., Chen, Y., Zhu, H., Li, J., Kim, J. K., & Leung, C. K. Environmental degradation of epoxy–organoclay nanocomposites due to UV exposure. Part I: Photo-degradation. Composites Science and Technology, Vol. 67, No. 15-16, 2007, pp. 3448-3456.

[31] Woo, R. S., Zhu, H., Leung, C. K., & Kim, J. K. Environmental degradation of epoxy-organoclay nanocomposites due to UV exposure: Part II residual mechanical properties. Composites science and technology, Vol. 68, Issue 9, 2008, pp. 2149-2155.

[32] Javaherdashti, R. How corrosion affects industry and life. Anti-corrosion methods and materials, Vol. 47, Issue 1, 2000, pp. 30-34.

[33] Schmidt, G, and Matthew M. Malwitz. Properties of polymer–nanoparticle composites. Current opinion in colloid & interface science, Vol. 8, Issue 1, 2003, pp. 103-108.

[34] Zare, Y. Study of nanoparticles aggregation/agglomeration in polymer particulate nanocomposites by mechanical properties. Composites Part A: Applied Science and Manufacturing, Vol. 84, 2016, pp. 158-164.

Fu, S. Y., Feng, X. Q., Lauke, B., & Mai, Y. W. Effects of particle size, particle/matrix interface adhesion and particle loading on mechanical properties of particulate–polymer composites. Composites Part B: Engineering, Vol. 39, Issue 6, 2008, pp. 933-961.